metals

MDPI

Article

Effect of Coiling Temperature on Microstructure and Properties of Ferritic-Bainitic Dual-Phase Steels

Zhengrong Li [1,*], Feng Zhou [2,3], Jinhai Liu [2,3], Lei Liu [2,3], Chuangwei Wang [1,4] and Zhengzhi Zhao [2,3,*]

[1] State Key Laboratory of Vanadium and Titanium Resources Comprehensive Utilization, Pangang Group Research Institute Co., Ltd., Panzhihua 617000, China; yjywcw@pzhsteel.com.cn
[2] Collaborative Innovation Center of Steel Technology, University of Science and Technology Beijing, Beijing 100083, China; d202110603@xs.ustb.edu.cn (F.Z.); g20209281@xs.ustb.edu.cn (J.L.); d202210629@xs.ustb.edu.cn (L.L.)
[3] Beijing Engineering Technology Research Center of Special Steel for Traffic and Energy, University of Science and Technology Beijing, Beijing 100083, China
[4] School of Materials Science and Engineering, Southwest Jiaotong University, Chengdu 610031, China
* Correspondence: yjylzr@pzhsteel.com.cn (Z.L.); zhaozhzhi@ustb.edu.cn (Z.Z.)

Abstract: In this study, a 780 MPa grade ferritic-bainitic dual-phase steel with excellent matching of strength-plasticity and formability was developed using thermomechanical control processing. Optical microscopy, Scanning electron microscopy, and Electron Backscatter Diffraction techniques were used to characterize the microstructure comprehensively, and the effects of coiling temperature on the microstructure, the strength-plasticity, and hole-expansion ratio of the test steels were thoroughly investigated. The results showed that the test steel had an excellent combination of ferrite and bainite at the coiling temperature of 520 °C, 23.7 and 76.3%, respectively, with a hole expansion ratio of 58.5 ± 2.8%. The uniformity of the microstructure was the key to obtaining a high expansion ratio in ferrite-bainite dual-phase steels. The test steels formed granular bainite at low-temperature coiling, while polygonal ferrite was promoted at high-temperature coiling. The effect of coiling temperature on grain size is small. Dislocations were redistributed during high-temperature coiling, resulting in a decrease in dislocation density. The higher elongation and hole expansion rate at higher coiling temperatures were attributed to increased polygonal ferrite content, reduced grain size, and enhanced TRIP effect. When coiling at low temperatures, the agglomeration of polygonal ferrite or granular bainite tends to result in a non-uniform distribution of the soft and hard phases of the matrix. At the same time, the strong texture parallel to the rolling direction has a significant difference in plasticity in different directions, leading to non-uniform deformation, which is liable to stress concentration, causing crack nucleation and extension in the hole expanding process, thus reducing the hole expansion performance.

Keywords: ferritic-bainitic duplex-phase steels; coiling temperature; the strength-plasticity; hole expansion ratio

Citation: Li, Z.; Zhou, F.; Liu, J.; Liu, L.; Wang, C.; Zhao, Z. Effect of Coiling Temperature on Microstructure and Properties of Ferritic-Bainitic Dual-Phase Steels. *Metals* **2024**, *14*, 365. https://doi.org/10.3390/met14030365

Academic Editor: Marcello Cabibbo

Received: 28 February 2024
Revised: 15 March 2024
Accepted: 19 March 2024
Published: 21 March 2024

1. Introduction

Advanced high-strength steels are typically bent at lower bending radii when used to manufacture complex parts, so the local stress-strain behavior of the steel becomes very important [1–4]. Hole expansion is one of the most important properties describing the formability of steel sheets, especially those used in the automotive industry [2,5]. Microstructural designs such as dual-phase steels and transformation-induced plasticity steels can achieve very high strength and elongation combinations, but the higher the strength, the higher the sensitivity to edge fracture and the lower the hole expansion rate, which hinders the effective implementation of the part design and stamping process [6–9]. The influence of microstructure on the formability of advanced high-strength steels is

critical. Sugimoto et al. [10] reported the tensile flangeability of a newly developed high-strength bainitic steel plate and showed that the strain-induced plasticity of the stabilized or carbon-rich retained austenite film during hole-expanding reduces the surface damage during punching and thus enhances the tensile flangeability. The strength-ductility-hole expansion ratio balance of Nb-containing steels is lower than that of Ti-containing steels, mainly due to the presence of large textural colonies and detrimental influence of MnS in Nb-containing low-carbon high-strength steels. In contrast, combining Ti and Nb can effectively improve the strength-ductility-expansion balance of advanced high-strength steels [11]. A proper process schedule facilitates microstructure control and is the best approach to improve formability. Cho et al. [9] investigated the effect of cooling on the formability of hot-rolled high-strength steels of TS 590 MPa grade. They showed that inhibiting cementite precipitation at grain boundaries (GBs) and reducing the hardness difference between the ferrite matrix and the bainite phase contributes to the excellent tensile flangeability of ferrite-bainite dual-phase steels. Microcrack formation and propagation are suppressed relative to conventional high-strength, low-alloy steels with ferrite and pearlite. At the same time, increasing the polygonal ferrite volume fraction improves the elongation of the test steel compared to the hot rolled steel sheet using conventional cooling mode. Wang et al. [12] investigated the effect of ultra-fast cooling after hot strip rolling on the hole expansion properties, and the results showed that the fine and homogeneous microstructure composed of ferrite and spheroidized cementite could improve the elongation value of the tested sheet by inhibiting the bonding of adjacent micro-voids, thus improving the hole expansion properties. Fang et al. [13] studied the effect of tempering temperature on the tensile and hole expansion properties of C-Mn dual-phase steel, and the results showed that the ultimate tensile strength and yield strength decreased with the increase of tempering temperature, and the elongation increased. At 200–300 °C tempering temperature, the hole expansion performance increases significantly, and when the tempering temperature is lower than 200 °C or higher than 300 °C, there is no significant difference in the hole expansion performance. Yoo et al. [14] investigated the Hall-Petch relationship between grain size and stretch-flangeability, and the results showed that reducing the grain size increases the hole expansion rate of advanced high-strength steels.

At present, the hole expansion ratio of 780 MPa grade advanced high-strength steels has been unsatisfactory, with the expansion ratio lower than 50%, and there is less literature on the study of the effect of coiling temperature on the microstructure, strength-plasticity, and hole expansion ratio of ferritic-bainitic duplex high hole expansion steels. Therefore, in this study, a ferritic-bainitic duplex steel of 780 MPa grade with a high hole expansion ratio was developed by using the thermomechanical control processing (TMCP), and the strength-plasticity and formability were analyzed by tensile and hole expansion tests at different coiling temperatures. The microstructure at different coiling temperatures was comprehensively characterized by optical, scanning electron, and electron backscattering diffraction techniques. The influence of microstructure on the strength-plasticity and formability of high-expansion steels was carefully investigated, which provides theoretical guidance for the industrialized production and application of 780 MPa ferritic-bainitic duplex phase steels.

2. Materials and Methods

The chemical compositions of the materials used in this study are shown in Table 1. The schematic diagram of the rolling procedure of the tested steel is shown in Figure 1. In order to ensure that the alloying elements are fully solid solution, the forging ingots will be heated to 1200–1250 °C above the heat preservation for 1 h after the end of the holding temperature through the mechanical vibration way to remove the surface of the iron oxide skin. The rolling process adopts the two-stage controlled rolling in the thermomechanical control processing (TMCP), i.e., through the austenite recrystallization region and the stage of the non-recrystallized region; on the one hand, the austenite grains are sufficiently refined to provide a refined microstructure for the phase transformation in the controlled

cooling process, and on the other hand, high-density dislocations and a large number of deformation bands are induced within the microstructure. The starting rolling temperature was set at 1100–1150 °C, and the finishing rolling temperature was 850–930 °C. After finishing rolling, three-stage cooling, i.e., water cooling-air cooling-water cooling, is used. The coiling temperatures were set at 480 °C and 520 °C, and the coiling time was 1 h. After the end of coiling, it was cooled to ambient temperature with the furnace.

Table 1. Chemical composition of the test steel.

C	Si	Mn	P	S	Nb + Ti + Mo	Fe
0.06–0.08	0.5–0.7	1.40–1.80	0.005–0.015	0.003–0.008	0.15–0.40	Bal.

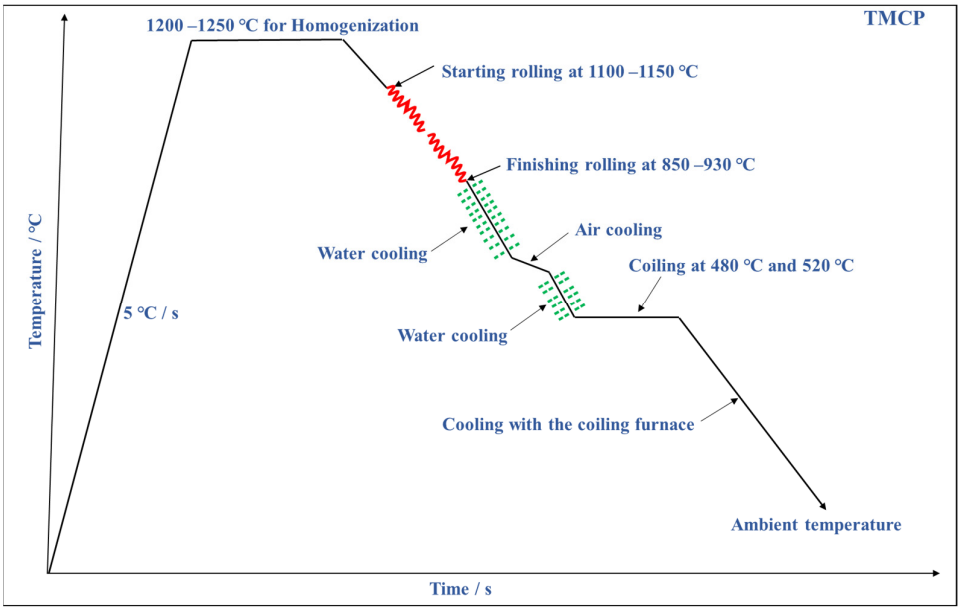

Figure 1. Schematic diagram of the TMCP for test steel.

Rolled plate due to preferred orientation, resulting in the anisotropy of its macroscopic mechanical properties, mainly manifested in the anisotropy of strengthening and yielding [15,16]. Anisotropy dramatically affects the distribution of stress and strain in the plate deformation process, the thickness of the thinning, and the formability of the plate. In order to ensure that the mechanical properties of the plate in all directions can reach the target, according to the standard GB/T 228.1-2021 along the 0°, 45° and 90° direction of the processing of tensile specimens, in each direction to take three tensile specimens for tensile experiments, tensile specimen processing schematic shown in Figure 2. The hole-expansion test is carried out according to the GB/T15825 standard. Three hole-expansion tests were carried out for each process. Figure 3 shows a schematic diagram of punching and hole-expanding. A 90 mm × 90 mm square plate was used with a 10 mm punch hole in the center. The hole was expanded using a conical punch with a 60° angle at the top until the hole's edge broke through the plate's thickness.

Grinding and polishing followed standard protocols for metallographic specimens. Etching used a 4% nitric acid-alcohol solution. Optical microstructures were examined with an Olympus Ols40-SU laser confocal microscope (Olympus, Tokyo, Japan). Scanning Electron Microscopy (SEM) utilized a ZEISS Gemini SEM 500 field emission microscope (ZEISS, Oberkochen, Germany) at 15 kV with a 10 mm working distance. Electron Backscatter Diffraction (EBSD) testing involved silicon carbide papers (400#, 800#, 1200#, 2000#, and 5000#) for grinding, followed by electrolytic polishing in 10% perchloric acid-alcohol. Electrolysis used 30 V and 1.5–1.8 A for 18–22 s. EBSD analysis employed a Symmetry S2 electron backscatter diffractometer (Oxford Instruments, Abingdon, UK) at 20 kV,

14.5 mm working distance, 0.5 µm step size, with a 70° tilted sample. Data was acquired at 105.65 Hz and processed with AztecCrysta.2.l software.

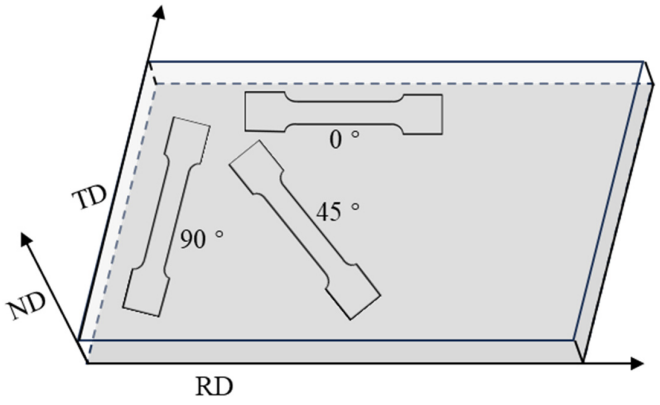

Figure 2. Tensile specimen machining schematic.

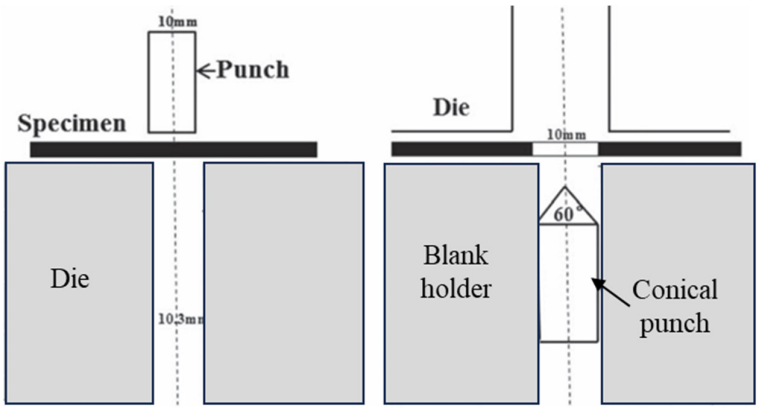

Figure 3. Schematic diagrams of the punching and hole-expanding test.

3. Results and Discussion

3.1. Tensile Properties, Hole Expansion Ratio, and Optical Microstructure Analysis

The mechanical properties of the test steels at different coiling temperatures were obtained by tensile and hole-expansion tests, as shown in Table 2. In the 0° direction, the difference in yield strength and tensile strength between the coiling temperatures 480 °C and 520 °C is small, but the total elongation of the coiling temperature 480 °C is higher than that of 520 °C. In the 45° and 90 °C directions, the yield and tensile strengths of coiling temperature 480 °C are higher than those of 520 °C. It is noteworthy that the hole expansion of 58.8 ± 2.8% at the coiling temperature of 520 °C is significantly higher than that of 44.2 ± 3.1% at the coiling temperature of 480 °C. For highly formable ferritic-bainitic dual-phase steels, the best strength-plasticity and hole expansion ratio matches were obtained for the tested steels at a coiling temperature of 520 °C.

Table 2. Comparison of literature summary related to high-strength weathering steels with this study.

CT/°C	Direction	Yield Strength/MPa	Tensile Strength/MPa	Total Elongation/%	Hole Expansion Ratio/%
480	0°	739 ± 11	815 ± 15	16.5 ± 0.8	44.2 ± 3.1
	45°	731 ± 9	794 ± 12	19.0 ± 0.6	
	90°	773 ± 11	845 ± 13	15.5 ± 0.8	
520	0°	745 ± 9	807 ± 14	14.5 ± 0.5	58.8 ± 2.8
	45°	684 ± 6	772 ± 10	20.0 ± 0.9	
	90°	723 ± 10	821 ± 15	18.0 ± 0.8	

The optical microstructures of the test steels at coiling temperatures of 480 °C and 520 °C are shown in Figure 4. As seen from the figure, the bright white structure is a polygonal ferrite [17,18]. Since both M/A island and cementite are black under an optical microscope, the black dot-like structure cannot be accurately identified by an optical microscope. However, it is worth noting that the black point-like structure exists within the grains and at the GBs. To obtain accurate microstructure information, see the SEM and EBSD characterizations below.

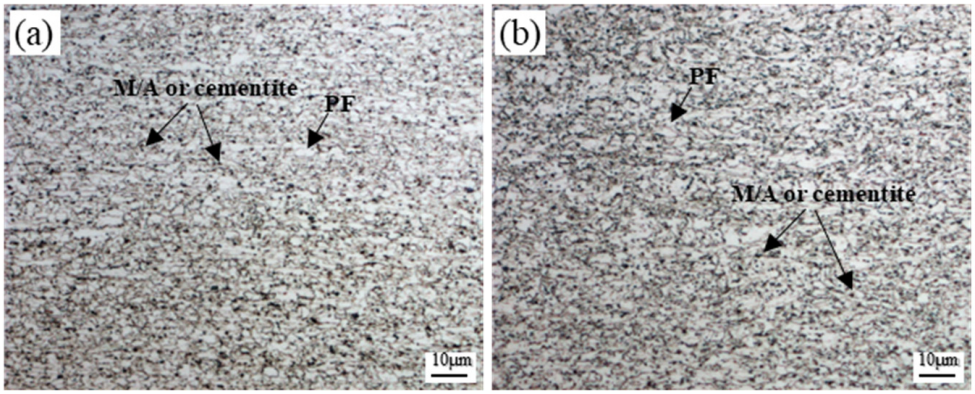

Figure 4. Optical microstructure of test steel at coiling temperatures 480 °C and 520 °C. (**a**) CT of 480 °C; (**b**) CT of 520 °C.

3.2. SEM Characterization

In high strength low alloy steels, the microstructures of the test steels were classified into polygonal ferrite and granular bainite based on transformation and morphology characteristics. PF has a very low dislocation density and an equiaxed shape, and the substructure is almost undeveloped. Granular bainite transforms at lower temperatures than PF and has coarser grains and substructures that contain islanded M/A components [18,19]. Based on these microstructural features, this study distinguishes between granular bainite and PF by combining SEM micrographs with the EBSD technique. The SEM micrographs of the test steels at coiling temperatures of 480 °C and 520 °C are shown in Figure 5. The microstructures of the test steels at the coiling temperatures of 480 °C and 520 °C consisted of polygonal ferrite and granular bainite. It can be determined that the black dot-like structures under the optical microstructure are M/A islands distributed at the ferrite GBs and within the grains. They are primarily elliptical, elongated, island-shaped, and irregularly shaped. Compared with the coiling temperature of 480 °C, the M/A islands were more uniformly distributed in the test steel at the coiling temperature of 520 °C. Granular bainite and PF are mixed in all steels, and granular bainite has a relatively large packet. However, it is challenging to completely distinguish granular bainite from PF using SEM alone. Analyzing and quantifying the phase fractions of GB and PF by XRD is impossible since both GB and PF belong to the BCC crystal structure.

3.3. EBSD Characterization

Granular bainite and polygonal ferrite are mixed in the microstructure, which cannot be distinguished in SEM only by morphological features and cannot be identified by XRD because both granular bainite and polygonal ferrite are BCC crystal structures. According to the literature [18–21], due to the different transition temperatures of PF and granular bainite, resulting in a significant difference in the misorientation angle of PF and granular bainite, it is possible to distinguish between granular bainite and polygonal ferrite by EBSD and the granular bainite and polygonal ferrite fractions can be quantitatively analyzed.

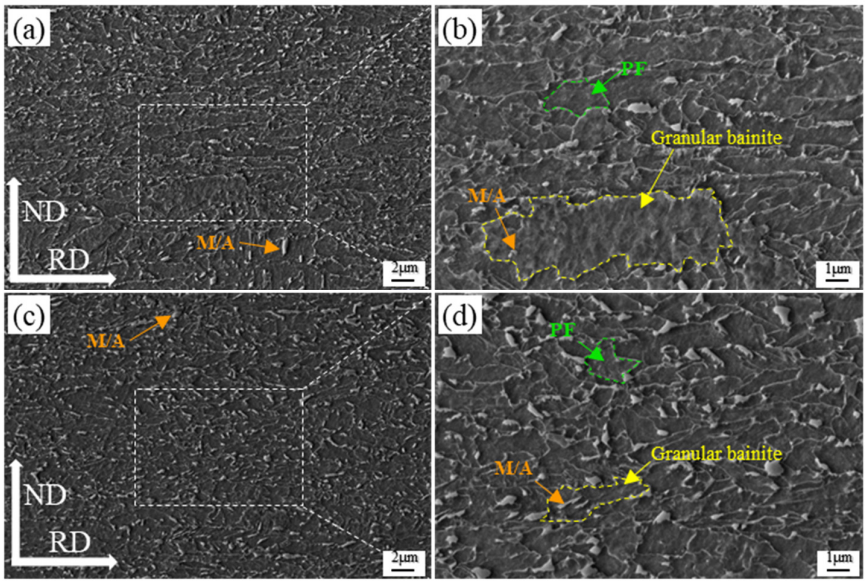

Figure 5. SEM micrographs of test steel at coiling temperatures of 480 °C and 520 °C: (**a**,**c**) are SEM micrographs at coiling temperatures of 480 °C and 520 °C, respectively; (**b**,**d**) are the local magnification of the rectangle region marked by the white line in (**a**,**c**), respectively.

According to the EBSD data analysis of the test steels by AztecCrystal software, the grain orientation spread (GOS), geometrically necessary dislocation (GND) density, and inverse pole figure e(IPF) of the two test steels at coiling temperatures of 480 °C and 520 °C were obtained, as shown in Figure 6. Figure 6(a1,b1) shows the grain GOS of the test steels at the coiling temperatures of 480 °C and 520 °C, respectively, which allows analyzing the presence of substructures within the grains by providing the degree of average misorientations between certain datum points. Granular bainite is defined by a misorientation angle of 15° or higher, while grains with a misorientation deviation of less than 3° are defined as PF [20–22]. In this study, high-angle grain boundaries (HAGBs) (>15°) and low-angle grain boundaries (LAGBs) (2–15°) are indicated by black and blue lines, respectively. The coarse microstructure containing many subgrains and the fine microstructure containing equiaxed grains are defined as granular bainite and PF, respectively [18,23], based on granular bainite and PF characteristics. Grains with an average misorientation angle of less than 3° are identified as PF, and those with an average misorientation angle of more than 3° are granular bainite (green represents polygonal ferrite). As can be seen from Figure 6(a1,b1), there are aggregates of granular bainite or PF present in the test steel at the coiling temperature of 480 °C, while the microstructure at the coiling temperature of 520 °C is uniformly distributed. In order to better demonstrate granular bainite and PF, data extraction and EBSD analysis were performed on the granular bainite and PF in the region I of Figure 6(b1), as shown in Figure 7. Green indicates PF, and red indicates granular bainite. It can be observed that there are few LAGBs within the PF, while the granular bainite has more substructures (Figure 7b). Neither granular bainite nor PF is significantly oriented (Figure 7a). It can also be noticed that the GND density within the granular bainite is higher than that of PF (Figure 7c). Figure 6(a2,b2) shows the GND density of the test steels at coiling temperatures of 480 °C and 520 °C, respectively. The average GND density at coiling temperatures of 480 °C and 520 °C is 10.77×10^{14} m^{-2} and 8.17×10^{14} m^{-2}, respectively. Figure 6(a3,b3) shows the IPF maps of the test steels at coiling temperatures of 480 °C and 520 °C, respectively, in which HAGBs (>15°) and LAGBs (2–15°) are indicated by black and white lines, respectively. The red grains of <001> in the organization were scaled using Image Pro 6.0 software, and the results showed that the grains of <001> in the test steels at coiling temperatures of 480 °C and 520 °C were 9.2% and 6.1%, respectively. At the coiling temperature of 480 °C, the <111> grain orientation of some of the grains was parallel to the rolling direction (yellow outline area in Figure 6(a3)).

In contrast, the grains of the test steel did not show any apparent preferred orientation at the coiling temperature of 520 °C (yellow outline area in Figure 6(b3)).

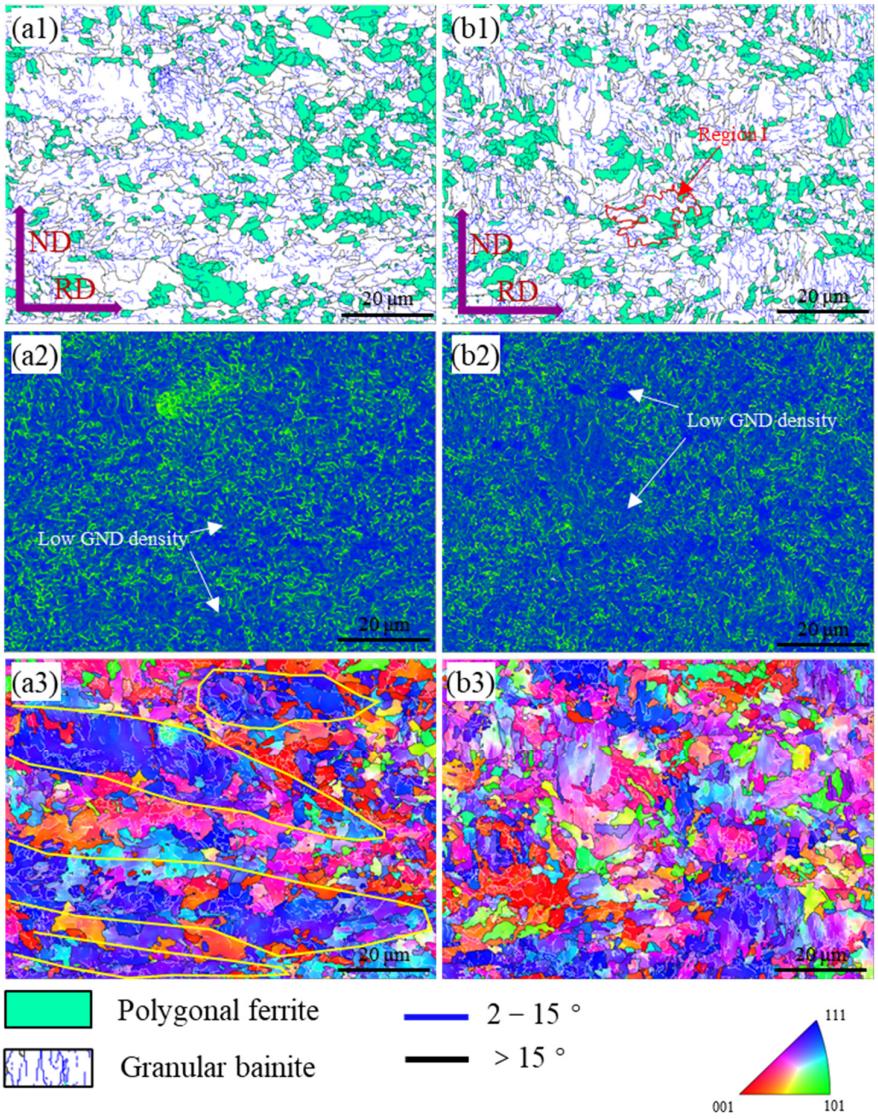

Figure 6. GOS, GNDdensity, and IPF maps of test steels at coiling temperatures of 480 °C and 520 °C. (**a1**–**a3**) 480 °C; (**b1**–**b3**) 520 °C; (**a1**,**b1**) are GOS maps, (**a2**,**b2**) are GND density maps, (**a3**,**b3**) are IPF maps.

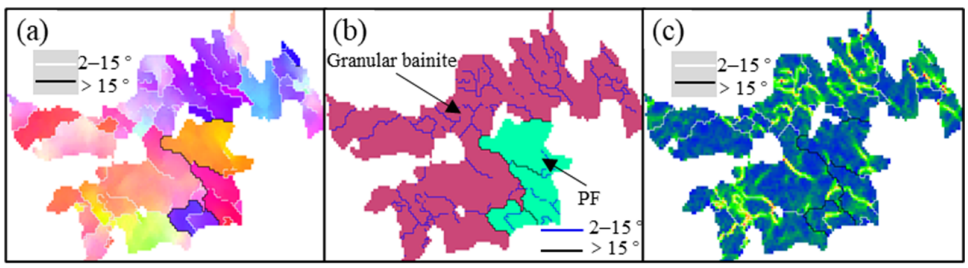

Figure 7. The fine structure of PF and granular bainite in region I. (**a**) IPF map; (**b**) GOS map; (**c**) GND density map.

The fractions of PF and granular bainite, the average grain size, and the proportion of misorientation angle were obtained by EBSD analysis, as shown in Table 3. The PF fraction of the test steel at the coiling temperature of 480 °C is lower than that of 520 °C,

but the average grain size of PF and granular bainite and the proportion of large-angle grain boundaries are slightly higher than that of 520 °C.

Table 3. Fraction of PF and grain bainite, average grain size, and proportion of misorientation angle of test steels at coiling temperatures of 480 °C and 520 °C.

CT/°C	Phase Ratio		Average Grain Size		Misorientation Angle/°	
	PF/%	Granular Bainite/%	PF/μm	Granular Bainite/μm	2–15°	>15°
480	19.2	81.8	1.42	4.70	47.4	52.6
520	23.7	76.3	1.35	4.66	48.8	51.2

3.4. Discussions

3.4.1. Effect of Coiling Temperature on Microstructure

Fast cooling after hot rolling obtained undercooled austenite with a large number of deformed substructures; polygonal ferrite began to form during the subsequent air-cooling process, and water cooling again to the coiling temperature, the undercooled austenite transformed into granular bainite, but a small proportion of the undercooled austenite was still retained without transformation. The lower the coiling temperature, the higher the content of granular bainite, and the higher the coiling temperature, the higher the content of retained undercooled austenite. At low-temperature coiling, the diffusion ability of carbon atoms is weak. However, the carbon atoms diffuse to the surrounding region during the isothermal phase transformation process. However, the degree of carbon enrichment is low, and it is impossible to form carbides. The carbon-rich austenite forms the M/A island in the subsequent cooling process, forming a predominantly granular bainite structure at the low-temperature coiling. As the coiling temperature increases, the diffusion ability of carbon atoms increases, and polygonal ferrite is formed. Therefore, the content of granular bainite at the coiling temperature of 520 °C is lower than that at 480 °C, while the content of polygonal ferrite is higher than that at 480 °C. It is well known that M/A islands consist of carbon-rich undercooled austenite partially transformed to martensite during cooling, with the balance retained as retained austenite [24]. Figure 8 shows the retained austenite at coiling temperatures of 480 °C and 520 °C (green color represents retained austenite). The content of retained austenite at the coiling temperature of 520 °C is 0.9%, which is higher than that at the coiling temperature of 480 °C. The main reason for this is that the higher the coiling temperature, the more stable the retained austenite is, so the retained austenite at a coiling temperature of 520 °C is higher than that at 480 °C.

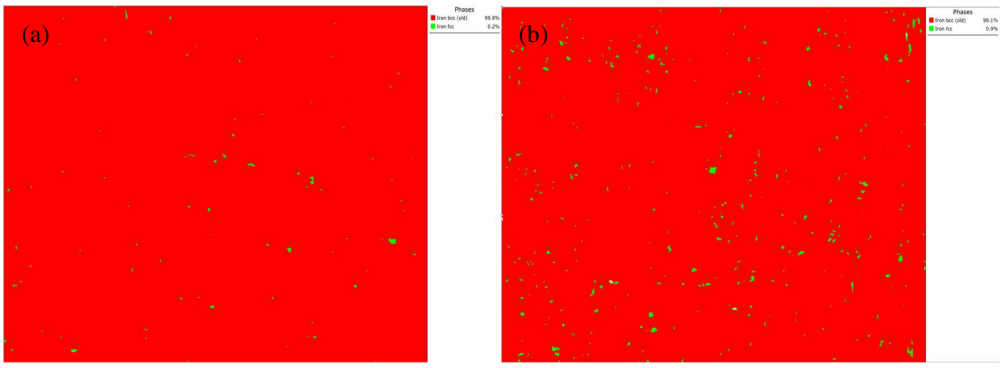

Figure 8. BCC and FCC crystal structures of test steels at coiling temperatures of 480 °C and 520 °C. (**a**) 480 °C; (**b**) 520 °C; red represents BCC crystal structure and green represents FCC crystal structure.

It has been proved that the grain size of steel obtained by the same rolling process and then by different coiling temperatures is almost the same [25,26]. Therefore, the effect of coiling temperature on grain size is small. It is well known that the dislocations generated

by the hot rolling and phase transformation processes will move and redistribute in the high-temperature coiling process. Different dislocations on the same slip surface can offset each other by climbing to decrease dislocation density. In contrast, irregular dislocations will be redistributed, and this distribution can significantly reduce the elastic distortion energy of dislocations. The higher the coiling temperature, the more advantageous it is for the movement and redistribution of dislocations. Therefore, the GND density at the coiling temperature of 520 °C is lower than that at the coiling temperature of 480 °C.

3.4.2. Effect of Coiling Temperature on the Strength-Plasticity and Hole Expansion Ratio

The yield and tensile strengths of the test steels at the coiling temperature of 520 °C are lower than those at 480 °C. On the one hand, this is because the content of granular bainite is higher at the coiling temperature of 480 °C, and thus the Phase transformation strengthening increment is higher. On the other hand, a low coiling temperature retains more dislocations generated by the rolling deformation and phase transformation process, leading to a higher dislocation strengthening at the coiling temperature of 480 °C than at 520 °C. It is worth noting that the test steel's total elongation and hole expansion ratio at the coiling temperature of 520 °C is higher than 480 °C. The main reason is that the ferrite content of the test steel at the coiling temperature of 520 °C is higher than that at the coiling temperature of 480 °C, ferrite belongs to the soft phase, and more ferrite participates in the deformation of the test steel at the coiling temperature of 520 °C during the deformation process. The smaller the average grain size, the more the plastic deformation can be distributed to more grains, and plastic deformation is more uniform, resulting in a slight stress concentration [14]. The tested steel at the coiling temperature of 520 °C has more retained austenite, and more retained austenite takes place in the TRIP effect during deformation, which further improves the plasticity of the material [10,27]. Therefore, the collaborative effect of ferrite content, average grain size, and TRIP effect contributed to the total elongation of the test steel at the coiling temperature of 520 °C, being slightly higher than that at 480 °C. The ferrite and granular bainite of the test steel at the coiling temperature of 520 °C were uniformly distributed. In contrast, the aggregation of granular bainite appeared in the test steel at the coiling temperature of 480 °C, resulting in an ununiform distribution of soft and hard phases in the matrix, which reduced the reaming performance of the test steel at the coiling temperature of 480 °C. In addition, it is shown that <001> has less grain slip system, which results in <001> grains being more prone to microcracking. At the same time, in the coiling temperature of 480 °C test steel in part of the grain in <111> parallel to the rolling direction of the strong texture, so in different directions of the plasticity of the difference is very large, resulting in non-uniform deformation, vulnerable to stress concentration, in the hole-expanding process, resulting in the nucleation and propagation of cracks, reducing the hole expansion performance [16,28]. Therefore, the hole expansion ratio of the test steel at the coiling temperature of 520 °C is higher than that of 480 °C.

4. Conclusions

In this study, a 780 MPa grade ferrite/bainite dual-phase high-hole expansion steel was developed using TMCP. The microstructure was fully characterized using OM, SEM, and EBSD characterization techniques. The effects of coiling temperature on microstructure, strength-plasticity, and hole expansion ratio were analyzed. The main conclusions are as follows:

(1) Excellent strong plasticity and a high hole expansion ratio were obtained for the test steel at the coiling temperature of 520 °C. The PF and granular bainite at the coiling temperature of 520 °C were uniformly distributed with contents of 23.7 and 76.3%, respectively. The retained austenite content at the coiling temperature of 520 °C was higher.

(2) The microstructure formed at low-temperature coiling is dominated by granular bainite, while high-temperature coiling is conducive to forming PF. The grain sizes

at 480 °C and 520 °C coiling temperatures are very close. The lower GND density at higher coiling temperatures is attributed to the favorable dislocation movement and redistribution during high-temperature coiling.

(3) The higher total elongation and hole expansion ratios of the test steels at higher coiling temperatures are attributed to the increased ferrite content, enhanced TRIP effect, and uniform distribution of the microstructure. The presence of polygonal ferrite or aggregates of granular bainite in the vascular organization of the test steels at low-temperature coiling resulted in an uneven distribution of soft and hard phases in the matrix. The strong texture parallel to the rolling direction, with a large difference in plasticity in different directions, leads to non-uniform deformation, which causes crack nucleation and propagation in the hole expansion process, thus reducing the hole expansion performance. Therefore, the use of reasonable coiling temperature to control the polygonal ferrite content and microstructure uniformity can effectively improve the forming properties of ferrite-bainite dual-phase steels.

Author Contributions: Conceptualization, Z.L. and F.Z.; methodology, L.L. and J.L.; software, L.L.; validation, C.W., J.L. and L.L.; formal analysis, F.Z. and Z.Z.; investigation, C.W.; resources, J.L.; data curation, F.Z.; writing—original draft preparation, F.Z. and Z.L.; writing—review and editing, Z.L. and Z.Z.; visualization, F.Z. and C.W.; supervision, Z.Z.; project administration, Z.Z. and Z.L.; funding acquisition, Z.L. and Z.Z. All authors have read and agreed to the published version of the manuscript.

Funding: This study was supported by The fifth batch of major science and technology projects in Panxi Experimental Zone: development and application of titanium micro-alloyed weather-resistant steel plates. Sichuan Science and Technology Program, China under Grant [No. 2021YFG0085].

Data Availability Statement: The original contributions presented in the study are included in the article, further inquiries can be directed to the corresponding authors.

Conflicts of Interest: Authors Zhengrong Li and Chuangwei Wang were employed by the company Pangang Group Research Institute Co., Ltd. The remaining authors declare that the research was conducted in the absence of any commercial or financial relationships that could be construed as a potential conflict of interest.

References

1. Prasad, K.; Venkatesh, B.; Krishnaswamy, H.; Banerjee, D.K.; Chakkingal, U. On the interplay of friction and stress relaxation to improve stretch-flangeability of dual phase (DP600) steel. *CIRP J. Manuf. Sci. Technol.* **2021**, *32*, 154–169. [CrossRef] [PubMed]
2. Cho, W.; Jeong, B.; Jeong, K.; Lee, S.; Kim, H.; Lee, J.; Kim, S.; Han, H.N. New approach to hole-expansion ratio in complex phase and martensitic steels: Understanding the role of punching damage. *J. Mater. Res. Technol.* **2023**, *26*, 837–849. [CrossRef]
3. Wu, Y.; Uusitalo, J.; DeArdo, A. Investigation of the critical factors controlling sheared edge stretching of ultra-high strength dual-phase steels. *Mat. Sci. Eng. A* **2021**, *828*, 142070. [CrossRef]
4. Costa, F.S.; Oliveira, F.C.; Barbosa, R. Enhancement of the stretch-flangeability of a cold-rolled dual phase steel intercritically annealed. *J. Mater. Res. Technol.* **2024**, *29*, 691–702. [CrossRef]
5. Qian, L.; Ji, W.; Sun, C.; Fang, G.; Lian, J. Prediction of edge fracture during hole-flanging of advanced high-strength steel considering blanking pre-damage. *Eng. Fract. Mech.* **2021**, *248*, 107721. [CrossRef]
6. Park, S.; Jung, J.; Cho, W.; Jeong, B.; Na, H.; Kim, S.; Lee, M.; Han, N. Predictive dual-scale finite element simulation for hole expansion failure of ferrite-bainite steel. *Int. J. Plast.* **2021**, *136*, 102900. [CrossRef]
7. Matsuno, T.; Sato, R.; Okamoto, R.; Mizumura, M.; Suehiro, M. Synergy effect of shear angle and anisotropic material ductility on hole-expansion ratio of high-strength steels. *J. Mater. Process. Technol.* **2016**, *230*, 167–176. [CrossRef]
8. Park, S.; Jung, J.; Kim, K.; Kim, H.; Kim, S.; Oh, K.; Lee, M.; Han, H. Practical microstructure-informed dual-scale simulation for predicting hole expansion failure of hyper-burring steel. *Int. J. Mech. Sci.* **2019**, *156*, 297–311. [CrossRef]
9. Choi, S.; Kim, E.; Kim, S. The micromechanical deformation behaviors of hot-rolled 590FB steel during hole-expansion test. *Int. J. Plast.* **2014**, *58*, 184–200. [CrossRef]
10. Sugimoto, K.; Nakano, K.; Song, S.; Kashima, T.; Huang, H.; Xu, G. Retained austenite characteristics and stretch-flangeability of high-strength low-alloy TRIP type bainitic sheet steels. *ISIJ Int.* **2002**, *42*, 450–455. [CrossRef]
11. Kamibayashi, K.; Tanabe, Y.; Takemoto, Y.; Shimizu, I.; Senuma, T. Influence of Ti and Nb on the strength-ductility-hole expansion ratio balance of hot-rolled low-carbon high-strength steel sheets. *ISIJ Int.* **2012**, *52*, 151–157. [CrossRef]
12. Wang, B.; Liu, Z.; Zhou, X.; Wang, G. Improvement of hole-expansion property for medium carbon steels by ultra fast cooling after hot strip rolling. *J. Iron Steel Res. Int.* **2013**, *20*, 25–32. [CrossRef]

13. Fang, X.; Fan, Z.; Ralph, B.; Evans, P.; Underhill, R. Effects of tempering temperature on tensile and hole expansion properties of a C-Mn steel. *J. Mater. Process. Technol.* **2003**, *132*, 215–218. [CrossRef]
14. Yoon, J.; Yu, H.; Lee, H.; Jung, J.; Kim, H. Effect of grain size on stretch-flangeability of twinning-induced plasticity steels. *Mat. Sci. Eng. A* **2018**, *735*, 295–301. [CrossRef]
15. Schmidova, E.; Klejch, F.; Sunilkumar, M. Development of anisotropy and strain hardening in damaged stamped parts made of IF steel. *Eng. Fail. Anal.* **2023**, *145*, 107015. [CrossRef]
16. Bakshi, S.; Javed, N.; Sasidhar, K.; Dhande, T.; Sharma, V.; Mukherjee, M. Effect of microstructure and crystallographic texture on mechanical anisotropy of Ti-Nb microalloyed hot rolled 800 MPa HSLA steel. *Mater. Charact.* **2018**, *136*, 346–357. [CrossRef]
17. Lepera, F. Improved etching technique for the determination of percent martensite in high-strength dual-phase steels. *Metallography* **1979**, *12*, 263–268. [CrossRef]
18. Yang, J.; Kim, D.; Lee, S.; Kim, Y.; Kim, W.; Sohn, S. Effects of granular bainite and polygonal ferrite on yield point phenomenon in API X65 line-pipe steels. *Mat. Sci. Eng. A* **2022**, *840*, 143006. [CrossRef]
19. Lee, S.; Lee, S.Y.; Lee, S.G.K.; Jung, H.G.; Hwang, B. Effect of strain aging on tensile behavior and properties of API X60, X70, and X80 pipeline steels. *Met. Mater. Int.* **2018**, *24*, 1221–1231. [CrossRef]
20. Kim, W.D.; Kim, W.K.; Bae, J.; Choi, W.; Kin, H.S.; Lee, S. Yield-strength prediction of flattened steel pipes by competing Bauschinger effect and strain hardening during pipe-forming. *Sci. Rep.* **2019**, *9*, 14002. [CrossRef]
21. Kim, W.D.; Sohn, S.S.; Kim, W.K.; Kim, K.S.; Lee, S. Study of Bauschinger effect of acicular ferrite and polygonal ferrite through ex-situ interrupted bending tests in API X80 linepipe steels. *Sci. Rep.* **2018**, *8*, 15598. [CrossRef]
22. Lee, S.G.; Li, L.; Lee, D.H.; Sohn, S.S.; Kim, W.G.; Um, K.K.; Kim, K.; Lee, S. Effects of Ni and Mn addition on critical crack tip opening displacement (CTOD) of weld-simulated heat-affected zones of three high-strength low-alloy (HSLA) steels. *Mat. Sci. Eng. A* **2017**, *697*, 55–65. [CrossRef]
23. Lee, S.G.; Sohn, S.S.; Kim, B.; Kim, W.G.; Um, K.K.; Lee, S. Effects of martensite-austenite constituent on crack initiation and propagation in inter-critical heat-affected zone of high-strength low-alloy (HSLA) steel. *Mat. Sci. Eng. A* **2018**, *715*, 332–339. [CrossRef]
24. Luo, X.; Xu, G.; Chen, X.; Wang, Z. Effect of undercooled austenite ausforming on the role of the M-A constituents in the CGHAZ toughness of the HSLA steels with bainite structure. *Mat. Sci. Eng. A* **2022**, *833*, 142571. [CrossRef]
25. Zhang, K.; Li, Z.; Sun, X.; Yong, Q.; Yang, J.; Li, Y.; Zhao, P. Development of Ti–V–Mo Complex Microalloyed Hot-Rolled 900-MPa-Grade High-Strength Steel. Acta Metall. *Acta Metall. Sin. (Engl. Lett.)* **2015**, *28*, 641–648. [CrossRef]
26. Kim, Y.W.; Song, S.W.; Seo, S.J.; Hong, S.; Lee, C.S. Development of Ti and Mo micro-alloyed hot-rolled high strength sheet steel by controlling thermomechanical controlled processing schedule. *Mater. Sci. Eng. A* **2013**, *565*, 430–438. [CrossRef]
27. Xu, X.; Xu, B.Y.; Chen, P.; Liu, R.D.; Wang, G.D.; Yi, H.L. Effect of austenite stability on the hole expansion behavior of 8-TRIP steels. *Mater. Today Commun.* **2020**, *24*, 101034. [CrossRef]
28. Verdeja, J.I.; Asensio, J.; Pero-Sanz, J.A. Texture, formability, lamellar tearing and HIC susceptibility of ferritic and low-carbon HSLA steels. *Mater. Today Commun.* **2003**, *50*, 81–86. [CrossRef]